MRS Advances
https://doi.org/10.1557/s43580-023-00513-5

ORIGINAL PAPER

Photoinduced excited-state dynamics in Co-doped $BaFe_2As_2$ superconducting films

Roman Kolodka[1] · Alexander Bartenev[1] · Ki-Tae Eom[2] · Jong-Hoon Kang[2] · Eric E. Hellstrom[3] · Chang-Beom Eom[2] · Armando Rua[1] · Sergiy Lysenko[1]

Received: 18 November 2022 / Accepted: 24 January 2023

Abstract

The nonlinear optical dynamics and structural transformation of Co-doped $BaFe_2As_2$ superconducting films demonstrate complex behavior within a broad range of temperatures. The angle-resolved light scattering conoscopy reveals the temperature-dependent structural transformation of the optimally doped $BaFe_2As_2$. Photoinduced excited states dynamics demonstrate the instantaneous formation of the nonequilibrium state of quasiparticles with its subsequent multi-step thermalization within several picoseconds. These transient processes show noticeable temperature dependence below superconducting transition point T_c, where photoinduced dynamics correlate with the surface morphology.

Introduction

Iron-based superconductors provide unique playgrounds for the exploration of their novel superconducting (SC) mechanisms [1–3] and exotic electronic and optical properties, such as nematicity [4, 5]. These intriguing properties emerge via the interplay of numerous degrees of freedom of charge, spin, and lattice. Thus, for example, quasiparticle relaxation dynamics in optimally doped high-temperature superconductor $(Ba,K)Fe_2As_2$ indicates the existence of precursor superconductivity above T_c that suppresses antiferromagnetism ($T_c \sim 28$ K, and spin-density wave (SDW) order emerges at ~ 85 K) [6].

$Ba(Fe_{1-x}Co_x)_2As_2$ is one of most attractive iron-arsenide-based superconductors due to its relatively high T_c, above 15 K. This material exhibits numerous exotic properties, including a tetragonal-to-orthorhombic structural phase transition, SDW, superconductivity, and electronic nematicity [7]. One of the most powerful methods to study nonequilibrium processes in SC materials is ultrafast spectroscopy. Time-resolved optical pump-probe transient reflectivity studies of $Ba(Fe_{1-x}Co_x)_2As_2$ superconductors show a bottleneck formation in the relaxation of the photoexcited quasiparticles below the tetragonal-to-orthorhombic structural transition temperature [8]. This bottleneck is associated with a partial charge-gap opening. It was found that in the SC state, an additional relaxation component appears in the optical signal. Observed saturation in the signal can be associated with complete nonthermal destruction of the SC state.

In this paper, we report the observation of nonequilibrium dynamics and optical and structural properties of Co-doped $BaFe_2As_2$ superconducting films. Special attention is focused on quasiparticle thermalization, electron and phonon scattering, and structural characteristics of the material near and below T_c. This work reveals the correlation between photoinduced-state dynamics, structural morphology, and formation of a superconducting state in optimally-doped $BaFe_2As_2$.

Materials and methods

Optimally-doped 80-nm-thick $Ba(Fe_{1-x}Co_x)_2As_2$ ($x = 0.08$) films were grown by pulsed laser deposition on both side polished $(La,Sr)(Al,Ta)O_3$ [LSAT] and $LaAlO_3$ [LAO] single crystalline substrates with epitaxial $SrTiO_3$ [STO] template buffer layer. To achieve TiO_2 terminated surface, STO template was etched by buffered hydrofluoric acid. Samples

✉ Roman Kolodka
roman.kolodka@upr.edu

1 Department of Physics, University of Puerto Rico, Mayaguez, PR 00681, USA

2 Department of Materials Science and Engineering, University of Wisconsin-Madison, Madison, WI 53706, USA

3 Applied Superconductivity Center, National High Magnetic Field Laboratory, Florida State University, Tallahassee, FL 32310, USA

Published online: 13 February 2023

were selected upon X-ray diffraction data and resistance measurements. The resistance was measured by four-point contact technique in a van der Pauw configuration. Ultrafast time-resolved pump-probe reflectivity measurements were performed with Spectra-Physics laser system operated at central wavelength of $\lambda = 800$ nm with pulse duration of 35 fs. A pump pulse of 8 mJ/cm^2 maximum fluence was used to trigger nonequilibrium processes in Co-doped $BaFe_2As_2$. A motorized rotary stage for $\lambda/2$ waveplate combined with linear Glan polarizer was used for the fine computer-controlled tuning of laser intensity. The estimated time for the complete thermal back-relaxation of an epitaxial film to its initial temperature after photoexcitation is a fraction of a microsecond. Therefore, possible film heating effects were minimized by using laser pulses with a sufficiently low repetition rate of 1 kHz.

Optical probe signal was detected by a fast photodiode and gated data processor. Temperature dependent optical measurements were conducted using a closed-cycle cryogen-free Janis cryostat. The supercontinuum laser (Leukos) was used as a white light source for transmission measurements. The spectra were acquired by Horiba ISA TRIAX320 spectrometer.

The angle-resolved hemispherical light scattering measurements were performed with a light scatterometer within a broad range of temperatures, from room temperature down to 6 K. The scatterometer uses aspherical reflective optics installed in a vacuum chamber with Janis cryostat in order to map the spatial distribution of the scattering indicatrix, providing the statistical information about multi-scale surface morphology as a function of temperature. Light scattering measurements were performed in cross-polarization geometry with crossed polarizer and analyzer as described elsewhere [9] to obtain conoscopy scattering indicatrices. These measurements allowed to detect material lattice transformation versus temperature.

Results and discussion

Figure 1a shows the transmittance spectra of Co-doped $BaFe_2As_2$ that were measured in the temperature range from 290 K down to 10 K. A Drude-Lorentz model was applied to fit transmission data within the near-infra-red (NIR) spectral region. The infrared region is crucial to superconductivity, as it covers both the superconducting gap and the energies of the excitations that lead to superconducting condensation. As can be seen from Fig. 1a, the experimental spectra and fitting curves within NIR 1100–1600 nm range show good coincidence. A discrepancy between experimental data and fitting curves within the visible region is attributed to the fact that the two spectral regions, visible and NIR, were measured at slightly different areas of the sample. Nevertheless, the main trend of the fitting in the visible range shows agreement with the experiment.

The cross-sections of spectra measured at certain fixed wavelengths are shown in Fig. 1b and c for $\lambda = 800$ nm and $\lambda = 1200$ nm, respectively. For the Low-T region, below 35 K, the transmittance was measured with higher resolution in temperature (circles). The main feature of the spectra

Fig. 1 **a** Transmittance spectra of $Ba(Fe_{1-x}Co_x)_2As_2$ ($x = 0.08$) in visible and NIR regions with fitting curves obtained from the Drude-Lorentz model. The inset shows the resistance of the sample versus temperature. **b** Temperature dependence of transmittance for $\lambda = 800$ nm and **c** for $\lambda = 1200$ nm

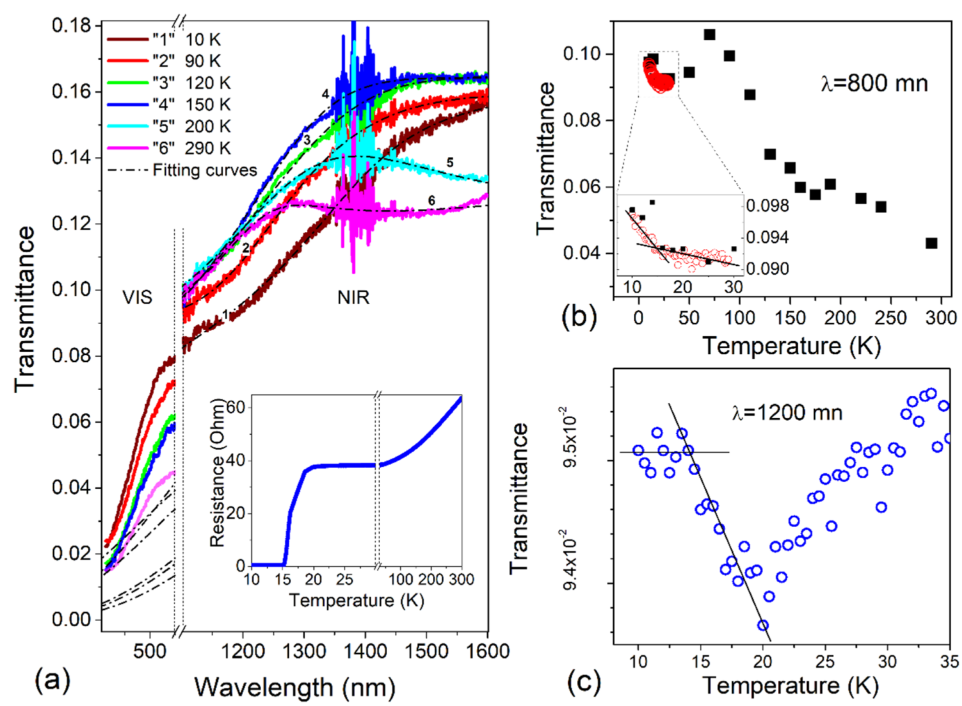

within this region is the noticeable rise of the signal as soon as the temperature drops below 20 K. At this point, it should be noted that the optical transmittance shows a good agreement with the temperature dependence of the resistance $R(T)$ of the sample at Low-T (inset in Fig. 1a). The $R(T)$ data shows that the SC transition starts at 20 K, and the material switches to a complete SC state below $T_c = 15.5$ K. Thus, as the temperature drops, optical transmittance after an abrupt rise at ~ 20 K experiences an additional change in the slope at 15 K for $\lambda = 800$ nm (Fig. 1b) and at 14 K for $\lambda = 1200$ nm (Fig. 1c) associated with complete formation of the SC sate.

In order to analyze the free-carrier components we use the Drude-Lorentz model to fit the optical transmittance spectra:

$$\epsilon(\omega) = \epsilon_\infty - \frac{\omega_p^2}{\omega^2 + i\omega/\tau} + \sum_{i=1}^{N} \frac{S_i^2}{\omega_i^2 - \omega^2 - i\omega/\tau_i}, \quad (1)$$

where ϵ_∞ is a dielectric constant at high energy, ω_p—plasma frequency, $1/\tau$—carrier scattering rate; the second and the third terms are the Drude and the Lorentz components, respectively. Drude-Lorentz model was applied to fit the optical transmittance spectra in order to demonstrate the contribution of a free-carriers component to the optical signal. The variations of $1/\tau$ and ω_p^2 with temperature for the Drude term are shown in Fig. 2a. The fraction of the Drude term (Fig. 2b) significantly prevails the Loretz's one in the whole measured temperature range. This indicates that the optical constants are mostly defined by free carriers of metallic Co-doped $BaFe_2As_2$.

The scattering rate $1/\tau$ was reduced by approximately 55–60% as the temperature dropped below 150 K. As the sample temperature decreases below 30 K the scattering rate shows relatively small but well-defined kink. It is believed that in Fe-based superconductors the carrier scattering rate is linked to T_c [10]. In standard BCS superconductors, the electron scattering rate is linked to the strength of the pairing interaction in the superconducting state. Therefore, it is likely that the carrier scattering changes near T_c and is directly related to the transition into the superconducting state. It starts slightly above T_c, at 30 K, and is likely related to lattice distortion, as will be shown below.

Previously, for pure undoped $BaFe_2As_2$ was shown, that the noticeable change of both carrier scattering rate and plasma frequency near ~ 150 K is associated with the spin density wave (SDW) transition. In the present work, we found qualitatively similar behavior of $1/\tau$ and ω_p^2 for Co-doped $BaFe_2As_2$ (Fig. 2b), where the SDW transition does not occur [11]. The sample shows typical thermal evolution of the resistance $R(T)$ for optimally Co-doped $BaFe_2As_2$ [12] without specific features at ~ 150 K associated with formation SDW. On the other hand, in angle-resolved scattering measurements, we observed an increase of the scattering signal within a relatively broad range of temperatures around ~ 150 K accompanied by a significant change of conoscopy scattering indicatrix between 108 and 186 K (Fig. 3). It should be noted that the isophote pattern of conoscopy images directly corresponds to the lattice symmetry of epitaxial film [9], and its temperature-dependent evolution indicates a lattice distortion, change of the film crystallinity, optical constants, and reconstruction of the surface geometry. It was found that several competitive transition processes near ~ 150 K alter the correlation length of the surface and optical properties. This fact suggests that the SDW transition in undoped $BaFe_2As_2$ could be initially triggered by temperature-dependent lattice distortion, while Co-doping shifts the temperature of SDW transition upon the distortion, and, at higher concentration of Co, completely suppresses the formation of SDW.

The bidirectional scatter distribution function (BSDF) of scattered light obtained within the hemisphere without a polarizer was used for the calculation of the surface autocorrelation function (ACF). The ACF was calculated by Fourier transform of BSDF data using the Gerchberg-Saxton error reduction algorithm that significantly reduces a numerical error, as described elsewhere [13]. Figure 3b and c show an example of the BSDF indicatrix and normalized ACF, respectively, measured in SC state at 6 K. The ACF defines a correlation of surface irregularities versus the translation

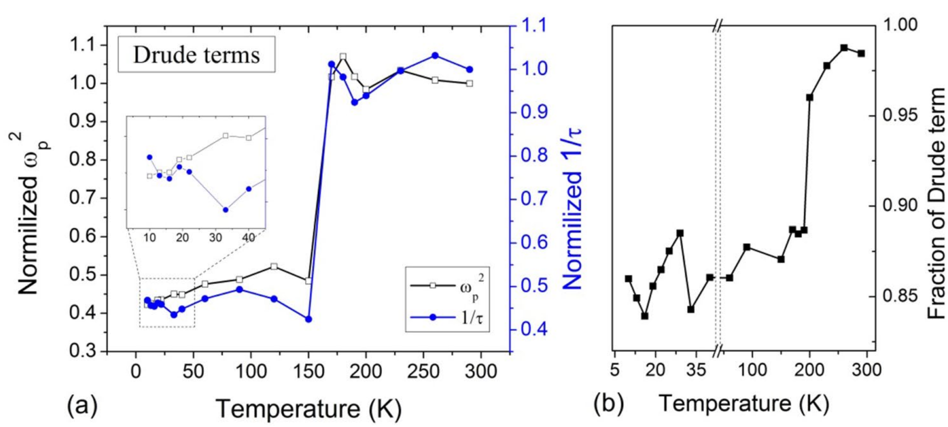

Fig. 2 Temperature dependence of **a** Drude terms and **b** Drude term fraction in the Drude-Lorentz model

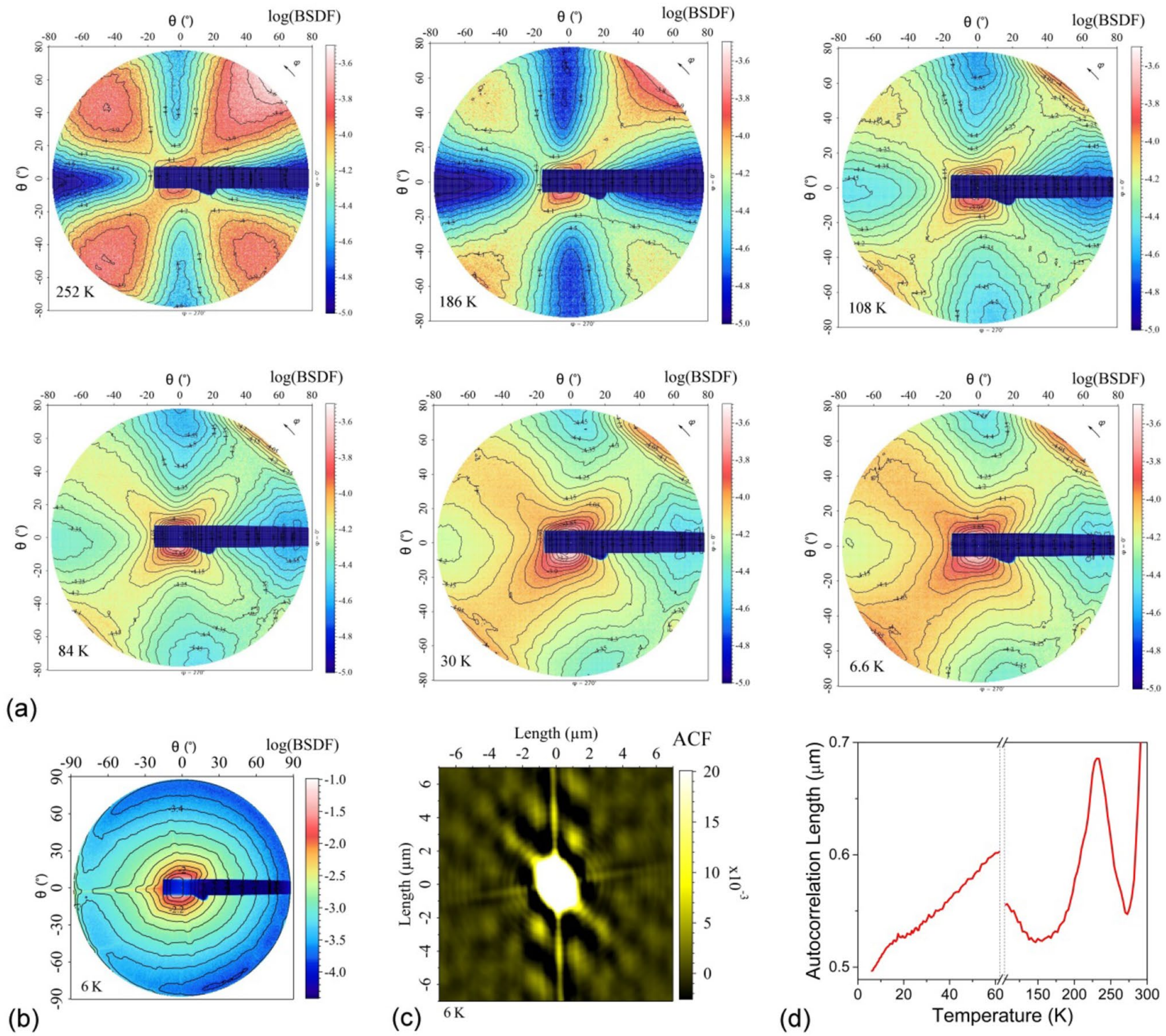

Fig. 3 **a** Diffraction conoscopy of $Ba(Fe_{1-x}Co_x)_2As_2$ ($x=0.08$) film: Evolution of the indicatrix shows gradual transformation of crystalline structure versus temperature. **b** BSDF indicatrix and **c** corresponded ACF at 6 K. **d** Surface autocorrelation length

length in the surface plane and was used for the calculation of surface autocorrelation length (ACL) for each sample temperature (Fig. 3d). ACL is one of the basic integral statistical characteristics of the surface and is defined as a distance where ACF drops in *e* times. Here it should be noted that the noticeable change in the ACL trend below 20 K indicates abrupt changes in surface morphology. This result remarkably correlates with SC transition in $BaFe_2As_2$, and can be associated with the anomaly of Fe–Fe sublattice near T_c [14].

Time-resolved measurements of transient reflectivity reveal a strong dependence of the excited-states dynamics on sample temperature, morphology, and laser excitation energy. Figure 4a demonstrates transient reflectivity variation $\Delta R/R(t)$ measured at the temperature of 8 K. Femtosecond photoexcitation demonstrates complex reflectance traces attributed to two distinct ultrafast processes: (i) instantaneous formation of the nonequilibrium state of quasiparticles with its subsequent thermalization within ~ 2 ps with characteristic time τ_1, and (ii) slower few-picoseconds phonon–phonon scattering characterized by time τ_2. Characteristic decay times were determined from a single-exponent fits at two different temporal scales: from 0 to 2 ps, and from 2 to 25 ps. In the NIR/visible frequency range, the $\Delta R/R(t)$ variation is generally considered to be dependent on the density of photoinjected quasiparticles [15, 16]. Temperature-dependences of τ_1 (Fig. 4b) and τ_2 (Fig. 4c) show a noticeable rise of these characteristic times as the temperature

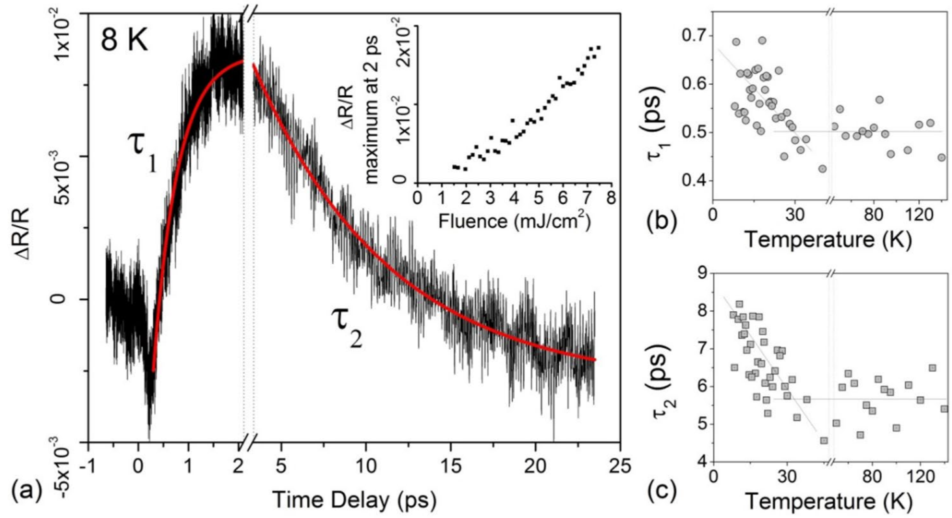

Fig. 4 **a** Time-resolved reflectivity ($\Delta R/R$) trace measured at 8 K. Inset shows $\Delta R/R$ maximum signal at 2 ps delay versus pump fluence. **b** Temperature dependences of relaxation time τ_1 and **c** time τ_2

lowers down below some threshold value ~ 30 K, slightly above T_c. The measured increase in the decay time in the SC phase is attributed to the suppression of the quasiparticle recombination process near T_c [17, 18]. The femtosecond timescale of the fast recombination confirms its electronic nature. The appearance of the peak, characterized by τ_1, represents the signature of the SC gap collapse [19]. The intensity of this peak increases with pump fluence, as shown in the inset of Fig. 4a.

The isophotes of diffraction conoscopy indicatrices (Fig. 3a) as well as the trend of the surface ACL (Fig. 3d), show noticeable qualitative change below 30 K. This behavior reveals additional structural change (lattice distortion) of Co-doped $BaFe_2As_2$ near T_c. Surprisingly, this temperature of structural transformation exactly coincides with the threshold temperature for characteristic time τ_1 (Fig. 4b) and τ_2 (Fig. 4c). Below this temperature electron–phonon and phonon–phonon scattering rates noticeably suppress, as the sample temperature diminishes. This indicates that the formation of a superconducting state in Co-doped $BaFe_2As_2$ is accompanied by additional lattice distortion.

Conclusions

In summary, femtosecond pump-probe optical spectroscopy reveals complex temperature-dependent nonlinear dynamics of optimally-doped $Ba(Fe_{1-x}Co_x)_2As_2$ ($x = 0.08$). These dynamics demonstrate a threshold behavior slightly above T_c. It is shown that the instantaneous photoexcitation of the nonequilibrium state of quasiparticles thermalizes within a few picoseconds, showing a threshold temperature behavior with a noticeable suppression of the electron–phonon and phonon–phonon scattering rates near and below T_c. The scattering polarization experiments herein demonstrate key features of $BaFe_2As_2$ at cryogenic temperatures in which nonlinear optical dynamics significantly depend upon film morphology. The angle-resolved light scattering conoscopy provides a unique opportunity to investigate the structural transformation of $BaFe_2As_2$ by optical means. The alteration of optical properties, conoscopy patterns, and surface autocorrelation length in the Low-T region, below ~ 30 K, along with superconducting transition indicates a noticeable alteration of the electronic density of states that also could be related to lattice distortion. Observed nonlinear optical dynamics correlate with the temperature dependence of the surface morphology near T_c and provide a new understanding of light-induced processes in the superconducting state of $BaFe_2As_2$.

Acknowledgments The work was supported at UPRM by the NSF Award# DMR-1905691. The work at University of Wisconsin–Madison (Thin film synthesis and characterization) was supported by the US Department of Energy (DOE), Office of Science, Office of Basic Energy Sciences (BES), under Award# DE-FG02-06ER46327.

Data availability The datasets generated during and/or analyzed during the current study are available from the corresponding author on reasonable request.

Declarations

Conflict of interest The authors state that they have no conflicts of interest.

References

1. K. Kuroki, S. Onari, R. Arita, H. Usui, Y. Tanaka, H. Kontani, H. Aoki, Unconventional pairing originating from the disconnected Fermi surfaces of superconducting $LaFeAsO_{1-x}F_x$. Phys. Rev. Lett. **101**, 087004 (2008)

2. T. Hanaguri, S. Niitaka, K. Kuroki, H. Takagi, Unconventional s-wave superconductivity in Fe (Se, Te). Science **328**, 474 (2010)
3. K. Okazaki, Y. Ota, Y. Kotani, W. Malaeb, Y. Ishida, T. Shimojima, T. Kiss, S. Watanabe, C.-T. Chen, K. Kihou, C.H. Lee, A. Iyo, H. Eisaki, T. Saito, H. Fukazawa, Y. Kohori, K. Hashimoto, T. Shibauchi, Y. Matsuda, H. Ikeda, H. Miyahara, R. Arita, A. Chainani, S. Shin, Octet-line node structure of superconducting order parameter in KFe_2As_2. Science **337**, 1314 (2012)
4. J.-H. Chu, H.-H. Kuo, J.G. Analytis, I.R. Fisher, Divergent nematic susceptibility in an iron arsenide superconductor. Science **337**, 710 (2012)
5. T. Shimojima, Y. Suzuki, T. Sonobe, A. Nakamura, M. Sakano, J. Omachi, K. Yoshioka, M. Kuwata-Gonokami, K. Ono, H. Kumigashira, A.E. Bohmer, F. Hardy, T. Wolf, C. Meingast, H.V. Lohneysen, H. Ikeda, K. Ishizaka, Lifting of xz/yz orbital degeneracy at the structural transition in detwinned FeSe. Phys. Rev. B **90**, 121111 (2014)
6. E.E.M. Chia, D. Talbayev, J.-X. Zhu, H.Q. Yuan, T. Park, J.D. Thompson, C. Panagopoulos, G.F. Chen, J.L. Luo, N.L. Wang, A.J. Taylor, Ultrafast pump-probe study of phase separation and competing orders in the underdoped (*Ba*, K)Fe_2As_2 superconductor. Phys. Rev. Lett. **104**, 027003 (2010)
7. P.C. Canfield, S.L. Bud'ko, FeAs-based superconductivity: a case study of the effects of transition metal doping on $BaFe_2As_2$. Annu. Rev. Condens. Matter Phys. **1**, 27 (2010)
8. L. Stojchevska, T. Mertelj, J.-H. Chu, I.R. Fisher, D. Mihailovic, Doping dependence of femtosecond quasiparticle relaxation dynamics in $Ba(Fe,Co)_2As_2$ single crystals: evidence for normal-state nematic fluctuations. Phys. Rev. B **86**, 024519 (2012)
9. N. Kumar, A. Rua, F.E. Fernandez, S. Lysenko, Ultrafast diffraction conoscopy of the structural phase transition in VO_2: evidence of two lattice distortions. Phys. Rev. B. **95**, 235157 (2017)
10. S. Ishida, M. Nakajima, Y. Tomioka, T. Ito, K. Miyazawa, H. Kito, C. H. Lee, M. Ishikado, S. Shamoto, A. Iyo, H. Eisaki, K. M. Kojima, S. Uchida, Strong carrier-scattering in iron-pnictide superconductors with highest T_c obtained from charge transport experiments. https://arXiv.org/1003.5039 (2010)
11. W.Z. Hu, J. Dong, G. Li, Z. Li, P. Zheng, G.F. Chen, J.L. Luo, N.L. Wang, Origin of the spin density wave instability in AFe_2As_2 (A= Ba, Sr) as revealed by optical spectroscopy. Phys. Rev. Lett. **101**, 257005 (2008)
12. P.C. Canfield, S.L. Bud'ko, N. Ni, J.Q. Yan, A. Kracher, Decoupling of the superconducting and magnetic/structural phase transitions in electron-doped $BaFe_2As_2$. Phys. Rev. B **80**, 060501(R) (2009)
13. S. Lysenko, V. Sterligov, M. Goncalves, A. Rua, I. Gritsayenko, F. Fernandez, Super-resolution in diffractive imaging from hemispherical elastic light scattering data. Opt. Lett. **42**, 2263 (2017)
14. M.Y. Hacisalihoglu, E. Paris, B. Joseph, L. Simonelli, T.J. Sato, T. Mizokawah, N.L. Saini, A study of temperature dependent local atomic displacements in a $Ba(Fe_{1-x}Co_x)_2As_2$ superconductor. Phys. Chem. Chem. Phys. **18**, 9029 (2016)
15. D. Dvorsek, V.V. Kabanov, J. Demsar, S.M. Kazakov, J. Karpinski, D. Mihailovic, Femtosecond quasiparticle relaxation dynamics and probe polarization anisotropy in $YSr_xBa_{2-x}Cu_4O_8$ (x=0, 0.4). Phys. Rev. B **66**, 020510R (2002)
16. N. Gedik, J. Orenstein, R. Liang, D.A. Bonn, W.N. Hardy, Gedik et al. Reply. Phys. Rev. Lett. **91**, 169702 (2003)
17. V.V. Kabanov, J. Demsar, D. Mihailovic, Kinetics of a superconductor excited with a femtosecond optical pulse. Phys. Rev. Lett. **95**, 147002 (2005)
18. N. Gedik, P. Blake, R.C. Spitzer, J. Orenstein, R. Liang, D.A. Bonn, W.N. Hardy, Single-quasiparticle stability and quasiparticle-pair decay in $YBa_2Cu_3O_{6.5}$. Phys. Rev. B **70**, 014504 (2004)
19. C. Giannetti, G. Coslovich, F. Cilento, G. Ferrini, H. Eisaki, N. Kaneko, M. Greven, F. Parmigiani, Discontinuity of the ultrafast electronic response of underdoped superconducting $Bi_2Sr_2CaCu_2O_{8+\delta}$ strongly excited by ultrashort light pulses. Phys. Rev. B **79**, 224502 (2009)